An application of the PEER PBEE framework to structures in fire

Engineering Structures 66 (2014) 100–115

Contents lists available at ScienceDirect

Engineering Structures

journal homepage: www.elsevier.com/locate/engstruct

An application of the PEER performance based earthquake engineering framework to structures in fire

David Lange [a,*], Shaun Devaney [b], Asif Usmani [b]

[a] SP Fire Research, Box 857, 501 15 Borås, Sweden
[b] BRE Centre for Fire Safety Engineering, Institute for Infrastructure and the Environment, School of Engineering, The King's Buildings, Mayfield Road, Edinburgh EH9 3JL, UK

ARTICLE INFO

Article history:
Received 3 May 2012
Revised 30 January 2014
Accepted 31 January 2014

Keywords:
Structures in fire
Performance based design
PEER
Fire engineering
Probabilistic analysis

ABSTRACT

The Pacific Earthquake Engineering Research (PEER) Center's Performance Based Earthquake Engineering (PBEE) framework is well documented. The framework is a linear methodology which is based upon obtaining in turn output from each of the following analyses: hazard analysis; structural analysis; loss analysis, and finally decision making based on variables of interest, such as downtime or cost to repair. The strength of the framework is in its linearity, its clear flexibility and in the consideration of uncertainty at every stage of the analysis. The framework has potential applications to other forms of extreme loading; however in order for this to be achieved the 'mapping' of the framework to the analysis of structures for other loading situations must be successful.

This paper illustrates one such 'mapping' of the framework for Performance Based Fire Engineering (PBFE) of structures. Using a combination of simple analytical techniques and codified methods as well as random sampling techniques to develop a range of response records, the PEER framework is followed to illustrate its application to structural fire engineering. The end result is a successful application of the earthquake framework to fire which highlights both the assumptions which are inherent in the performance based design framework as well as subjects of future research which will allow more confidence in the design of structures for fire using performance based techniques.

This article describes the PEER framework applied to structural earthquake design then follows the framework from start to completion applying suitable alternative tools to perform each stage of the analysis for structures in fire.

1. Introduction

Building structures are designed to offer a desired level of resistance to fire in order to satisfy the fire safety requirements of "insulation, integrity and stability". Insulation and integrity are required for vertical as well as horizontal separation which may be provided by the floor slab or other non-load bearing elements and stability which is provided by the structure as a whole, where the primary objective is safe evacuation of occupants and secondary objectives may include property protection. The allowability of alternative solutions to prescriptive fire safety design by many national standards and approvals bodies means that objectives for life safety may be met in a number of ways. This offers a far wider spectrum of possible design solutions than is available under prescriptive regulation [1]. Secondary criteria such as expected losses, downtime and the social impact of a fire are not necessarily fully addressed by these alternative solutions however these should be of interest to all stakeholders in a project since alternative solutions will have varying degrees of impact on the consequences of a fire post-evacuation. Further, significant cost savings with reference to property damage may be achieved by employing alternative solutions, however the full assessment of the effect of this requires the consideration of multiple design solutions and not a single alternative solution as is commonly investigated in industry. Since fire is such a low probability, high consequence event with considerable costs associated with protection the use of performance based design frameworks accounting for multiple solutions is particularly attractive, accounting for not only the primary objectives but also any secondary objectives.

The basic elements of a performance based design framework are therefore defined in such a way as to allow the user freedom to compose any solution to the problem, allowing also the freedom to employ new techniques and technologies as they become available. The objectives must be clearly stated at the outset of the project, and any design solution which fulfils these objectives whilst

* Corresponding author. Tel.: +46 10 516 5000.
E-mail address: david.lange@sp.se (D. Lange).

http://dx.doi.org/10.1016/j.engstruct.2014.01.052
0141-0296/

still adhering to the performance targets of the design framework should be permitted. It should be noted that although the targets in terms of life, property and business protection may remain similar to those prescribed in prescriptive design codes, these targets should remain independent of their prescriptive counterparts. In summary, performance based design is based upon three main criteria [2]:

- Definition of the objectives of the design process.
- Investigation of the alternative designs available to meet the objectives.
- Reliability and risk assessment of alternatives to select the most efficient solution.

The concept of performance based engineering therefore allows a broad spectrum of design solutions to be developed for different problems and evaluated based upon their individual merits by allowing a quantification of the impact – either in terms of qualitative or quantitative 'risk' – of an event. An example of performance based design applied to structural fire engineering is provided in [3].

In order to fully realise performance based design, it is necessary to account for uncertainty and probabilistic response in the analysis of structures. Research on the estimation of probabilistic response of structures to fire includes the use of analytical or first order reliability models [4,5] as described in the Eurocode basis of structural design [6]; as well as Monte Carlo techniques [7]. Some examples use a risk assessment method, such as that defined in [8] using fault tree analysis, for determining suitable fire scenarios for use in the study but do not consider the variation in the structure [9], while others vary the structure and the mechanical loading [10]. Random sampling can be both computationally expensive and time consuming since the number of calculations required increases with the number of variables in the system. To reduce the large number of analyses required for Monte-Carlo analysis, other work on the reliability of life safety and suppression systems in fire proposes the use of response surface modelling and linear regression techniques to identify critical variables for reliability estimation and then employ iterative algorithms to reduce the number of calculations required [11,12]. These techniques lead to less computationally expensive analyses than traditional Monte Carlo techniques. Stern-Gottfried and Rein developed a methodology for travelling fires which lends itself strongly to probabilistic methods [13,14]. In their method a family of fires is developed based on fuel distribution and burning rate within a compartment. Each of these fires is equally possible within their method and the sensitivity of a structure to the different fires should be determined when evaluating the safety of the structure.

In the majority of cases, however, performance based structural fire engineering will stop short at a risk assessment – where the supposed consequences of the fire on the structure are often presented as a subjective likelihood of, e.g. structural failure. While this allows a comparative assessment of the response of a design to a standard solution; in order to achieve a fully performance based approach, including considerations of sustainability and design optimisation, the expression of performance goals in fully quantifiable economic terms – for example an expected dollar loss – is necessary. These definitions are vital to the acceptance of performance based structural engineering for extreme loading as anything other than an occasional ad hoc alternative to prescriptive guidance. Numerous examples exist of frameworks applying these concepts to earthquake engineering and this field appears to be more mature in this respect than structural fire engineering. This paper uses one example of a framework which was originally devised for the design of earthquake resistant structures and applies it to structures in fire.

2. The PEER framework

2.1. Introduction

The PEER PBEE (Pacific Earthquake Engineering Research Center Performance Based Earthquake Engineering) framework provides a clearly defined process which outputs quantitative measures to assess the performance of a building system subject to ground excitation during an earthquake [15]. The framework is based across three calculation 'domains': the Hazard Domain; the Structural System Domain; and the Loss Domain. These domains are linked by so-called 'pinch variables'. The calculation follows a linear process of calculation of variables representing the severity of an event (Intensity Measure (IM)), the structural response to the event (Engineering Demand Parameters (EDPs)), and estimation of damage and resulting losses incurred (Damage Measures (DMs) and Decision Variables (DVs)) in the loss domain. The framework is expressed as a triple integral, Eq. (1).

$$gDV = \iiint \underbrace{P[DV|DM]P[DM|EDP]}_{\text{Loss Domain}} \overbrace{P[EDP|IM]}^{\text{Structural System Domain}} \mathrm{d}DM\mathrm{d}EDP \underbrace{\mathrm{d}gM}_{\text{Hazard Domain}} \tag{1}$$

where g denotes the annual rate of an event, and P denotes the complementary cumulative distribution function of an event, with $P[X|Y]$ denoting the conditional probability of $X \geq x$ given $Y = y$ occurs.

Implicit in the form of the equation is the assumption that each of the variables in the analysis is conditionally independent. That is to say that the probability distribution of, e.g. the EDP, is independent of the probability distribution of the IM and the engineering response is dependent solely upon the one variable chosen to represent the intensity measure. For example, given an event which may be characterised by a number of intensity measures such as peak ground acceleration or displacement – where one parameter is chosen to represent the intensity measure the distribution of the EDP is therefore assumed to be independent of the choice of IM variable. This is clearly an erroneous assumption. In structures in fire the form of the structure and the features of the compartment or room of origin directly influence the definition of the fire scenario (unless only the most simple nominal fire models are used such as the ASTM or ISO fire curve). This means that the expression of an EDP variable against alternative single IM's may result in different distributions. However, by careful selection of the intensity measure which is chosen to represent the hazard the effect of this may be limited. This is the subject of on-going work by the authors of this paper. The general process of the PEER framework is shown in Fig. 1. This follows the linear progression of Hazard Analysis, Structural Analysis, Damage Analysis and Loss Analysis, with each stage linked by the pinch variables. The intention of the framework is to return metrics of annual expected losses for a given structure based on the likely recurrence and magnitudes of the hazard of interest.

Fig. 2 shows the framework presented schematically. Fig. 2a illustrates the relationship between the performance of the system and the intensity measure based on the damage analysis and the engineering demand parameter. In this instance the illustration shows a case where only the hazard analysis is non-deterministic and all other variables are deterministic, the engineering system domain is also a simple function of the hazard domain with no additional influences from alternative possible intensity measures, similarly the loss domain is a function of the engineering system, i.e. EDP = f(IM) and DM = f(EDP). This is almost a trivial case since the unknown in the solution arises solely from the hazard domain. Fig. 2b shows the impact that introducing uncertainty and

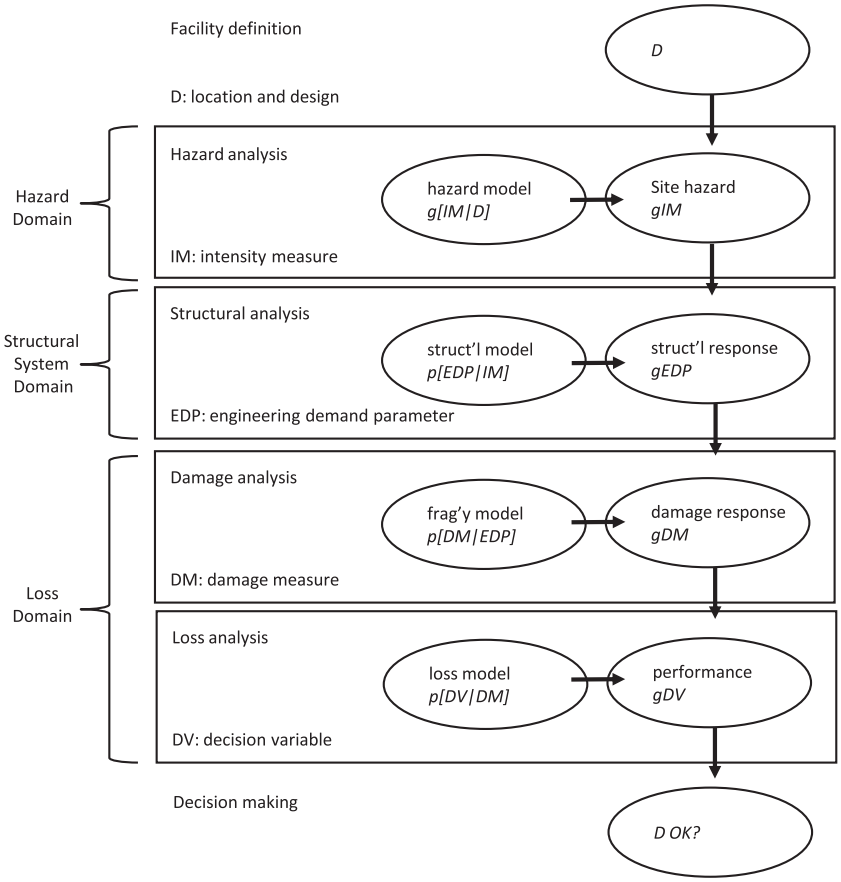

Fig. 1. PEER analysis methodology (adapted from Porter [3]).

additional variables in the subsequent modules has on the result. In this case, the intensity measure which may lead to some target performance has a wide range, and the frequency of occurrence of this intensity measure is also relatively unknown. Fig. 2c shows the results of the integration of each of the analyses which leads to the expression of the frequency of exceeding either a minimum engineering demand parameter, or a damage state leading to a loss.

The framework is comprehensively reported in a number of references, for example Porter [16] provides a simple and easily followed description of the framework and its components. Additional information and background reading may be found on the PEER website. The individual modules of the PEER framework are outlined in the following sections although for a more detailed description other references should be consulted.

Examples of the PEER framework adapted to and applied to other extreme loading cases exist, for example applied to wind engineering as a performance based wind engineering framework [17], to blast engineering [18], and to hurricane engineering [19]. Deierlein and Hamilton [20] also propose an application of the PEER framework to fire engineering. This is a straightforward mapping of the PBEE framework to fire however there is no example of application provided.

2.2. Hazard domain

The hazard analysis results in the output of the intensity measure. The intensity measure is defined as a single or vector parameter that defines the event intensity and which quantifies the rate or probability of exceeding an intensity per year. In PEER PBEE the calculation of the intensity measure follows broadly the methodology employed in probabilistic seismic hazard analysis (PSHA), although where PSHA results in a rate or a probability of exceeding an intensity measure, the calculation required for the PEER framework results in a mean *annual* probability of exceedance.

In the resulting hazard curves used in examples of the PEER framework the variable chosen to represent the intensity of the event seems to be typically the peak ground acceleration, however alternative variables may be used to measure the magnitude of an event including ground displacement, ground motion frequency, duration of the ground motion, etc. A sensitivity analysis should typically be carried out to investigate the sufficiency of IM's for alternative EDP's [21].

The intensity measure is illustrated by the hazard curve, which is defined by the frequency of exceeding an intensity measure. This is equal to the probability of exceeding a given value of intensity measure given that an earthquake of a given magnitude has occurred, multiplied by the statistical rate of occurrence of an earthquake of the given magnitude. For a single magnitude event the intensity measure hazard curve is given by the following equation.

$$gIM = r_n P(IM) \tag{2}$$

where r_n is the rate of occurrence of the event.

For intensity measure hazard curves comprised of either multiple fault lines or multiple magnitude events, the total hazard curve is comprised of the maximum of all the likelihoods of exceeding the intensity measure for each of the scenarios. This analysis is locationally dependent. That is to say that for each location there may be a number of fault lines at varying distances and the intensity of an event will vary with the distance to the fault line. The hazard analysis therefore needs to be carried out for the location of interest.

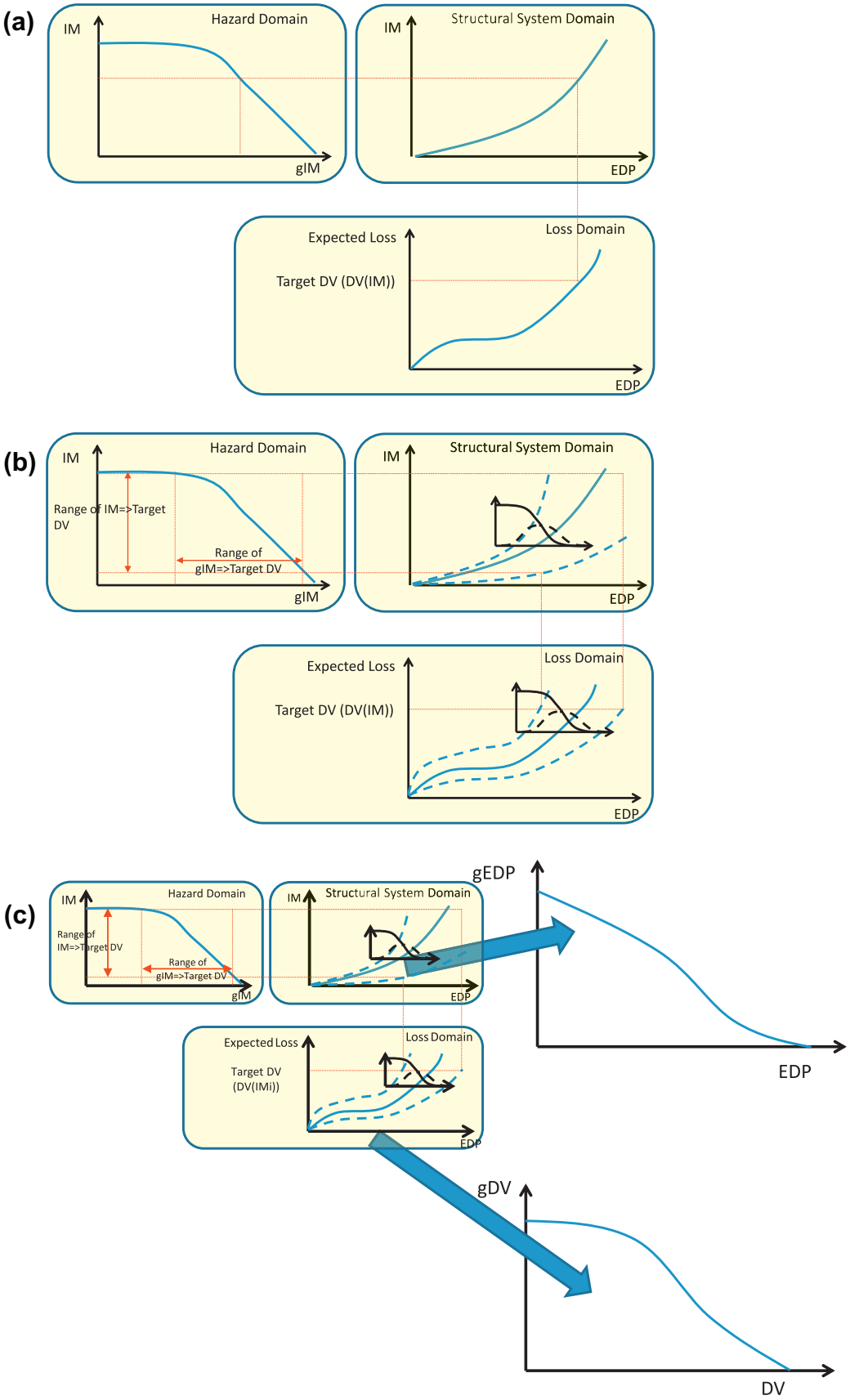

Fig. 2. Schematic of the PEER framework: (a) where the structural analysis, damage analysis and the loss analysis are deterministic the relationship between the hazard and the consequences is easily traced; (b) where there is some uncertainty associated with any of the modules which follow the hazard analysis then the range of intensity measures, and event frequencies, which give rise to some target performance in terms of loss may be quite considerable; and (c) in this instance the structural system and the loss domains must be integrated in accordance with the triple integral of Eq. (1) to give the frequency of exceeding the target performance.

2.3. Structural system domain

The structural analysis uses the records of perturbation from a database of earthquake records to determine the response of the structure for each of the records. This may be the same set of records that was used to perform the hazard analysis, however it does not have to be so long as the resulting EDP can be expressed as a function of the IM which is used to define the severity of the event. The output from the structural analysis is a probabilistic measure of the response of the structure which will be related to the damage analysis which follows in subsequent stages of the framework. For example, for typical examples of the framework applied to earthquakes the engineering demand parameter studied is the inter-storey drift. The structural analysis should reflect the response of the structure across the whole vector of the Intensity Measure.

The engineering demand parameter is expressed as a hazard curve, similar to the intensity measure, defined as a vector parameter which again permits the quantification as a Poisson process of the rate of exceedance given the intensity measure hazard curve.

$$gEDP = \int P(EDP|IM)dgIM \tag{3}$$

Uncertainty in the response of the structure to a seismic event means that the structural response to a given intensity measure has some probabilistic distribution associated with it and this may be included in the structural analysis to ensure that it is included in the demand parameter hazard curve.

As stated, in examples of the PEER PBEE framework, the structural analysis often relies on a catalogue of earthquake records to determine the likely response given a peak ground acceleration (or other intensity measure) [22]. However the calculation of the structural response is based on the contents of entire records of earthquakes and not just the variable which is chosen to reflect the intensity measure. By representing the intensity of the earthquake as a function of a single variable it is assumed in the probabilistic calculation which follows that the distribution of the response of the structure is independent of any variation in the other variables which may be chosen to reflect the intensity and which may also affect the structure. This is a drawback of the framework. In future applications of the framework the sensitivity of the engineering demand parameter to the intensity measure is an important consideration when choosing the variable to represent the IM.

The structural analyses carried out to determine the probabilistic distribution of demand parameters for given intensity measures do not need to be deterministic and should normally include probabilistic aspects to describe uncertainty in the model such as uncertainty in material properties or other factors which may affect structural response.

2.4. Loss domain

Following the structural analysis, fragility functions for predetermined damage measures should be specified or derived based on the range of structural responses arising from the hazard. In the case of, for example, earthquake analysis using the PEER framework; a common example of damage measure is damage associated with cracking of the separating walls in a building following an earthquake. Occurrence of small cracks which can be repaired are damage measure 1, larger cracks in the gypsum board are damage measure 2. Damage measure 3, in this example, may refer to damage to the framing of the stud wall in addition to damage to the plasterboard, requiring replacement of the entire separating wall assembly. Each of these damage measures has a fragility function associated with it which reflects the probability of this degree of damage occurring given a value of the engineering demand parameter. Other examples of damage measures may include concrete cracking in a reinforced concrete frame; evolution of plastic hinges in frames, or any other damage which may occur in a building subject to some kind of perturbation. The fragility function for an individual damage measure reflects the probability of a damage measure given the magnitude of the engineering demand parameter, i.e. $P(\mathrm{DM}|\mathrm{EDP})$.

Loss analysis is based on the damage measure which occurs. Each damage measure is associated with a cost to repair which again has some probabilistic distribution given the extent of the damage. The loss analysis therefore relies on the results of the damage analysis to derive consequence curves based on whether or not a damage state exists given the EDP hazard curve. The loss being considered may include, for example, down time or cost to repair. In PBEE consequence curves are used to provide an estimate of the annual impact of an earthquake for, e.g. budgetary reasons in order to allow developers to better assess the impact of performance based structural engineering decisions on their own project.

3. The PEER framework adapted to structural fire engineering

For earthquake engineering as opposed to fire engineering, a relative wealth of independent records of earthquake events exists with libraries and databases of earthquakes in different regions being available. This is facilitated by the independence of the earthquake and the corresponding ground motion from the structure – the variables which are of interest in determining the ground motion intensity from the libraries of available data may be limited to only the distance from the fault line of the facility and the soil/ground conditions at the site. Conversely, the evolution of a fire in a structure is almost always dependent upon the form of the structure as well as its features. It may therefore be necessary to develop a suitable catalogue of fires bespoke to each structure, to determine the intensity measure and the engineering demand parameters.

3.1. Hazard domain

In examples of the PEER framework there are a number of different factors which may be taken as measures of the intensity, although as said typically peak ground acceleration seems to be used. In fire, several parameters have been historically considered to be measures of fires ‘intensity’; duration, for example, as a measure of fire resistance implies that the duration of burning is a measure of the intensity. However when considered in the context of real fires, the duration alone is insufficient and the fire severity may also be described in terms of parameters such as, for example: rate of increase in the temperature in a compartment, duration of the steady burning phase, or peak temperature, heat flux, etc.

At this stage, peak compartment temperature is taken as the intensity measure in this article, this was chosen based on ad hoc analysis done during the writing of this paper and there is no suggestion that this is a fully adequate indicator of fire intensity and ongoing work includes studies to determine the most appropriate intensity measure for engineering demand parameters of interest. The variation in response of the structure to the catalogue of fires is dealt with within the calculation of the engineering demand parameter.

In order to derive the intensity measure curve a procedure for probabilistic fire hazard analysis is mapped to the procedure for probabilistic seismic hazard analysis, as described below.

3.1.1. Probabilistic definition of fire models

As mentioned, applications of the PEER framework may rely on a catalogue of representative earthquakes such as those described in [22] which are used to develop a set of characteristic responses to the loading. Work by Koo [23] details a methodology for developing a set of possible fire curves for a given compartment geometry based on a set of random input variables. Although application of Koo's method provides a realistic set of compartment temperature–time curves of suitable number for stochastic purposes it is computationally intensive. Nevertheless, the approach of random sampling to derive a number of fire scenarios based on physical limitations of the compartment of fire origin has been shown to be a suitable means of deriving a large bespoke catalogue of fires.

For this example, a Eurocode parametric fire curve is used for the determination of the temperature within the compartment. This fire curve is a nominal temperature–time curve representative of a compartment fire which is commonly used in industry. The equation allows the variation of the fuel load, opening factor and the thermal inertia of the compartment linings when determining the compartment temperature. As well as being commonly used in industry the fire curve is also straightforward and is not resource intensive to construct. As well as the small degree of variability of the inputs, the output is also simple and includes both a heating phase of non-predetermined duration and peak temperature and a linear cooling phase. Local variations in temperature within the compartment are not considered within the model. The calculation required is deterministic within the Eurocodes and therefore at least one of the parameters needs to be varied in order to provide the necessary group of fire records for further analysis.

Of the parameters which may be varied, the fuel load and the actual opening factor as opposed to the available opening factor have considerable uncertainty associated with them. Variability in the thermal inertia of the wall linings, once the construction of these have been determined, is arguably less uncertain and will be ignored here.

The Structural Eurocodes (EN 1991-1-2: 2002) [24] give basic data on the distribution of fire load densities for various occupancy classifications. Average fire loads are listed along with the 80% fractile fire load (assuming Gumbel distribution). Using this data and the background documents to the Eurocodes allows for the construction of the entire distribution of fuel loads within a compartment [25]. This is shown in Fig. 3 for a typical office building.

The CDF and the PDF of the fire load have been created by taking the average fire load density as 420 MJ/m^2 and the coefficient of variation as 0.3. They show that the average fire load presents a relatively large probability of occurrence. It should be noted that this is not the probability of a structurally significant fire occurring but the likelihood of the fire load that will be present within the room of origin.

Independent distributions also exist for the opening factor, for example the Joint Committee on Structural Safety (JCSS) probabilistic model code [26] gives an expression for a truncated log-normally distributed variable which is used as a modifier for the maximum opening factor. However the opening factor is arguably not independent of the fuel load. Higher temperatures are likely to produce larger opening factors as more glass breaks, and this in turn could result in a decrease in the temperature, or conversely further increase in temperature as more unburnt fuel vapours can burn with more air available. The Eurocode parametric fire seems to imply an opening factor which is equal to the maximum available, within certain limits, and the variation of opening factor with time or temperature is outside of the scope of the parametric fire model. Nevertheless, in order to more effectively capture the potential fire scenarios which may occur based on a parametric fire the maximum opening factor will be modified by the corresponding reduction factor obtained from the JCSS model code. The opening factor is therefore determined using the following equation:

$$F = F_{max}(1 - \xi) \tag{4}$$

where F is the opening factor for calculation and F_{max} is the maximum available opening factor based on the compartment geometry, ξ is a random log-normally distributed parameter with mean 0.2 and standard deviation 0.2 which is truncated at 1.

Using random sampling techniques, vectors of the opening factor (assuming a compartment geometry) and the fuel load are defined. Based on these vectors a sample library of fire records can be generated.

Having created the family of fires, the distribution of possible values of the peak compartment temperature is given by Eq. (5) assuming that the distribution of the intensity measure may be approximated by an extreme value distribution. For this example, the cooling phase of the fire is ignored and peak compartment temperature is taken as the intensity measure.

$$p(T_{max}) = \frac{ze^{-z}}{\beta} \tag{5}$$

where p is the probability density function, and $z = e^{-\frac{T_{max}-\mu_{Tmax}}{\beta_{Tmax}}}$, given that μ_{Tmax} and β_{Tmax} are the mean and the shape factor of the distribution of peak compartment temperatures observed.

Integrating this, Eq. (6), gives the probability of exceeding a given temperature given that a fire occurs:

$$P(T_{max}) = \int_{T_{max\,i}}^{\infty} \frac{e^{-\frac{T_{max}\cdot\mu_{T\,max}}{\beta}} e^{-e^{-\frac{T_{max}\cdot\mu_{T\,max}}{\beta}}}}{\beta} dT_{max} \tag{6}$$

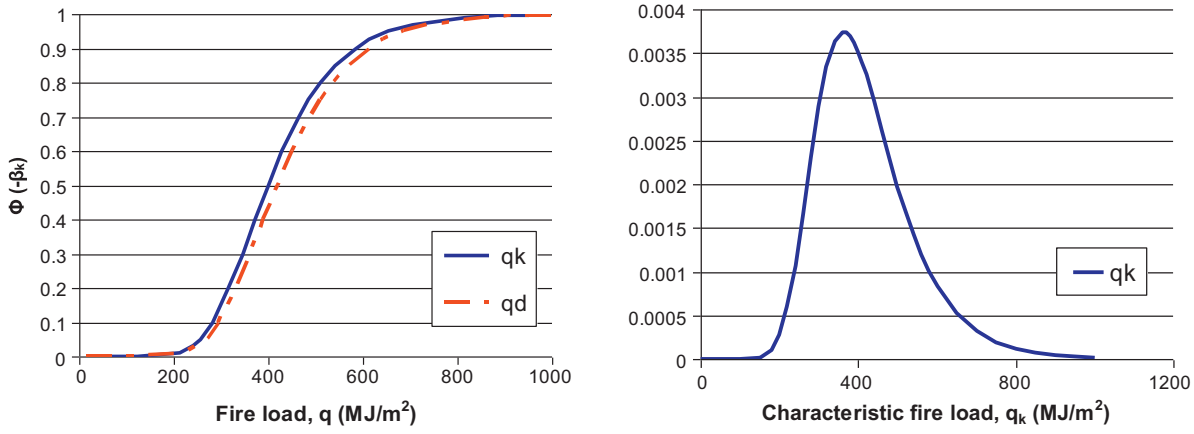

Fig. 3. Cumulative distribution function and probability density function of the fire load as a Gumbel distribution.

In order to obtain the annual rate of exceedance of the temperature, this probability must be multiplied by the annual rate of occurrence of a fire in the building.

The natural fire safety concept [27] proposes the frequency of structurally significant fires to be:

$$r_{fi} = A_{fi} \times p_1 \times p_2 \times p_3 \times p_4 \quad (7)$$

where r_{fi} is the rate of a structurally significant fire occurring, p_1 is the probability of severe fire affecting the occupants and the standard public fire brigade per m^2 floor area per year; p_2 is the probability of the fire brigade failing to extinguish the fire, p_3 is a reduction factor which allows for notification by means of automatic fire detection system, p_4 is the probability of sprinklers extinguishing the fire, and A_{fi} is the area of the fire compartment.

- For a typical office building, p_1 is quoted as being in the range of 2–4e−7/m^2/year.
- p_2 is dependent upon the type of firemen and upon the response time. For example if a response from professional fire fighters can be expected between 10 and 20 min after activation of the alarm then p_2 is quoted as being 0.1.
- p_3 is dependent upon the type of alarm installed. For example the use of smoke alarms gives a p_3 of 0.0625, whereas heat alarms give a reduction factor of 0.25. Automatic transmission of the alarm to the fire brigade will result in a further reduction factor of 0.25 being applied.
- p_4 is dependent upon the type and quality of sprinkler installed. A normal sprinkler system will give a reduction factor of 0.02.

The annual rate of exceeding the intensity measure is given by the product of the annual rate of occurrence of a fire and $P(IM)$, given by Eq. (6), where T_{max} is chosen to represent the intensity measure.

3.1.2. Example of the intensity measure calculation

The structure to be used in the example is based on a sub-assembly from the SCI document 'Comparative Structure Cost of Modern Commercial buildings (Second Edition) [28]. The floor plan of the building indicating the compartment where the sub-assembly is located is shown in Fig. 4.

The compartment is 15 m by 15 m and comprises 4 bays of the structure. Although the layout of the building as proposed in the SCI document is open plan, the compartment size is limited in this analysis for simplicity.

Based on the compartment boundary as outlined above, the total area of the compartment boundaries is assumed to be 612 m^2. The following assumptions with regards to available openings are also made: the height of the window openings is assumed to be 1.2 m and the total area of openings is estimated to be 46.6 m^2. The opening factor is varied according to the JCSS probabilistic model code. Using a medium fire growth rate corresponding with the fire growth rate of office buildings and the fuel load distribution as discussed above, a catalogue of parametric fires was developed based on 3000 random samples of fuel load and opening factor. The resulting catalogue of fires is shown in Fig. 5. The two extremes of fire scenario are also indicated in Fig. 5 – a long-cool fire and a short-hot fire [29].

Using the figures above the probability of a structurally significant fire occurring in the compartment may be estimated. Ignoring the possible effect of sprinklers since these are not included in the design according to the SCI guide and assuming remote monitoring of the smoke detection system is in place the annual recurrence of a fire in the compartment, p_{fi}, is $r_{fi} = 2.4e{-}7 \times 0.0625 \times 0.25 \times 225 = 1.05e{-}6$.

It should be noted that this ignores any statistical relationship between the likelihood of fires occurring and the geographical location. For comparison, if we consider the likelihood of a fire starting anywhere within the building, which is 18,000 m^2 floor area the frequency is 8.4e−5 fires per year. These figures compare favourably with the frequency for occurrence of fires in office buildings quoted in the JCSS probabilistic model code of 1e−6 per year.

Recalling the assumption that the distribution of maximum compartment temperature can be described by an extreme value distribution the maximum compartment temperature, T_{max}(°C), as intensity measure is plotted in Fig. 6 below as well as the corresponding hazard curve.

3.2. Structural system domain

3.2.1. Fire–structure interaction

The temperature distribution through the depth of a section may be described as a thermal gradient, $T_{,z}$, and a uniform temperature increase, ΔT, using an idealised temperature distribution through the sections depth [30], as shown in Fig. 7.

The effect of these two heating parameters on a structure may be described as a thermal force and a thermal moment [31]. These are both defined for composite sections in Eqs. (8) and (9) below:

$$N^T = EA\alpha\Delta T \quad (8)$$

$$M^T = E\frac{d^3}{12}\alpha T_{,z} \quad (9)$$

where E is Young's modulus of elasticity, A is the area of the section, d is the depth of the section and α is the coefficient of thermal expansion. The value of both of these parameters is dependent upon the heat transfer through the section as well as upon the material properties of the section. The fire–structure interaction model is based on an analysis of the section to determine the equivalent temperature increase and the equivalent through depth thermal gradient.

The stress distribution throughout the composite member is dependent on the structural form of the member, the temperature distribution through the member and the mechanical loading. The analysis procedure is simplified by dividing the cross section into horizontal slices. The stress and strain values can then be calculated at the boundaries of these slices.

Heat transfer analysis is carried out using standard techniques. Where the steel is unprotected the temperature may be calculated using a stepwise function as outlined in Eurocode 3 [32], Eq. (10):

$$\Delta T_s = k_{sh}\frac{H_p/A}{c_s\rho_s}\dot{h}_{net}\Delta t \quad (10)$$

where ΔT_s is the change in temperature of the steel, using a lumped capacitance approximation, over time interval Δt; k_{sh} is a correction factor for the shadow effect; H_p/A is the ratio of the heated perimeter to the cross-sectional area of the section; c_s is the specific heat capacity of the section and ρ_s is the density of the section; $\dot{h}_{net}$ is the design value of heat flux per unit area of the section.

Where the steel is protected, codified methods also exist to allow the temperature of steel to be calculated [32], Eq. (11).

$$\frac{k_i/d_i}{c_s\rho_s}\frac{H_p}{A_s}\frac{T_g - T_s}{1+\theta/3}\Delta t - (\exp(\phi/10) - 1)\Delta T_g = \Delta T_s \quad (11)$$

where $\phi = \frac{c_i\rho_i}{c_s\rho_s}d_i\frac{H_p}{A_s}$

The heat transfer through concrete is a marginally more complicated matter. For the standard fire, Eurocode 2 [33] contains prescribed isotherms which may be used for the determination of temperature distribution through a concrete section. However for the parametric fire curve chosen a 1-d heat transfer analysis may be used. This is achieved through the use of the procedure de-

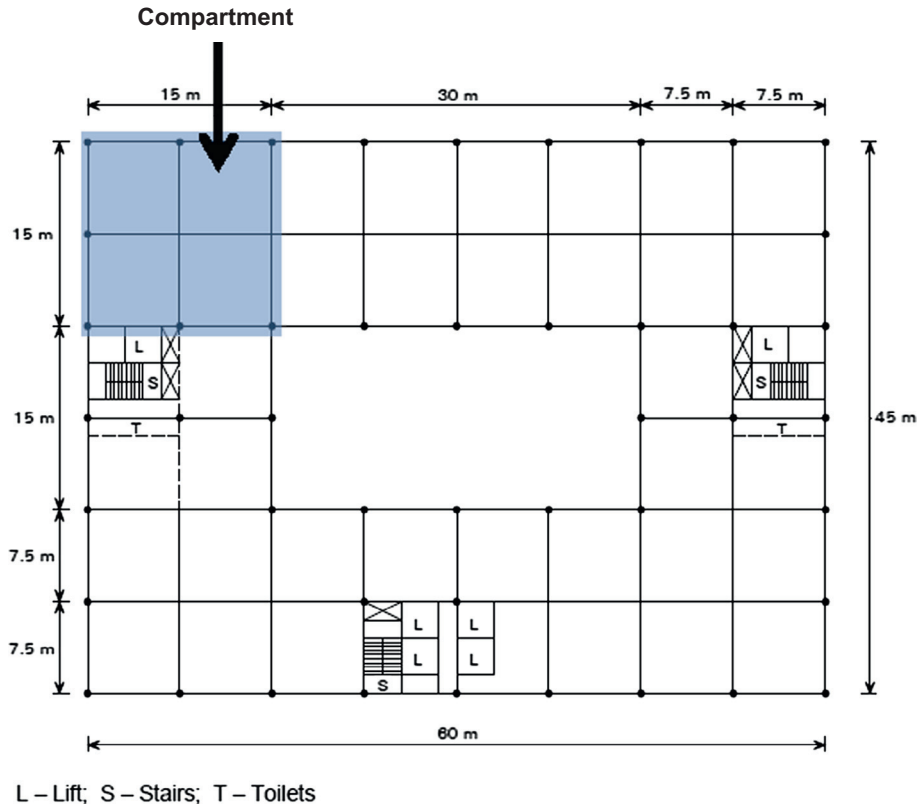

Fig. 4. The floor area and the location of the compartment used in the analysis.

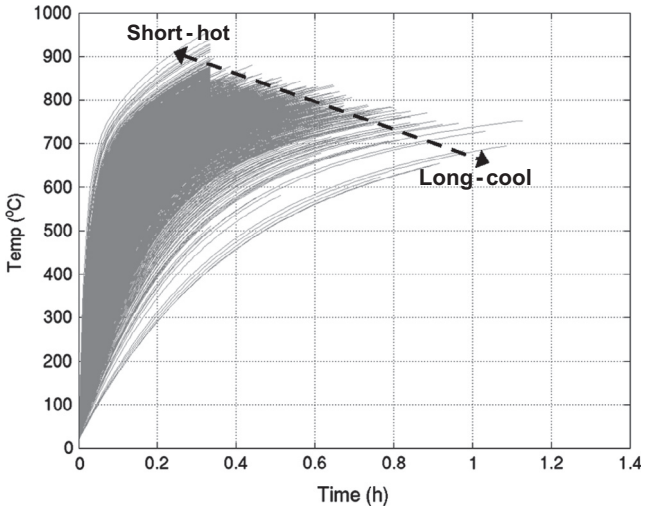

Fig. 5. Individual records of compartment temperature.

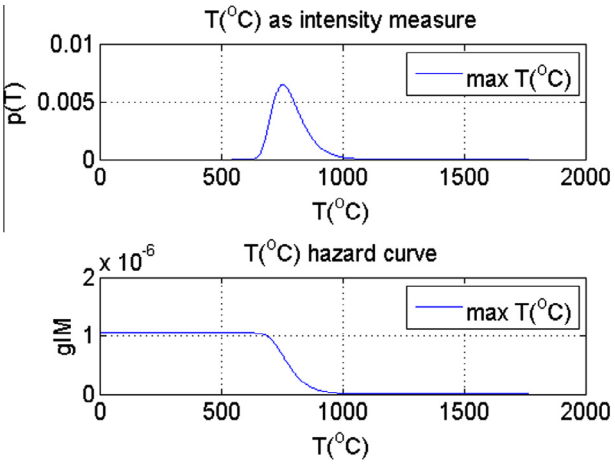

Fig. 6. Equivalent peak compartment temperature as intensity measure and the corresponding hazard curve.

scribed by Drysdale [34]. Although this ignores the latent heat of evaporation of the water within the concrete it is deemed to be suitable for use in this case due to its simplicity.

Lamont et al. describe the response of a structure to a long-cool and a short-hot fire [29] (both of the extremes shown in Fig. 5), Fig. 8. The short-hot fire results in a higher peak temperature and, due to the short duration of the heating phase of the fire, a larger thermal gradient within the structure. This causes large thermal moments which induce bowing within a structure and a tensile force within, for example, a composite section. Correspondingly, a long-cool fire will have a much more uniform temperature distribution through a section. This will cause large compressive forces to develop within an element exposed to fire which must be accommodated by the surrounding structure. It should be noted that the tensile or compressive forces in these cases will only form where there is some restraint to lateral translation at the ends of the beam. The different thermal response of composite structures to a long-cool and a short-hot fire are illustrated in Fig. 9. This figure shows the more uniform temperature throughout the depth of the composite section during a long-cool fire as opposed to the steeper gradient of temperature through the depth of the short-hot fire.

3.2.2. Structural system model

The response of the floor system to fire is based on the assumption that the floor system acts in a tensile membrane mechanism.

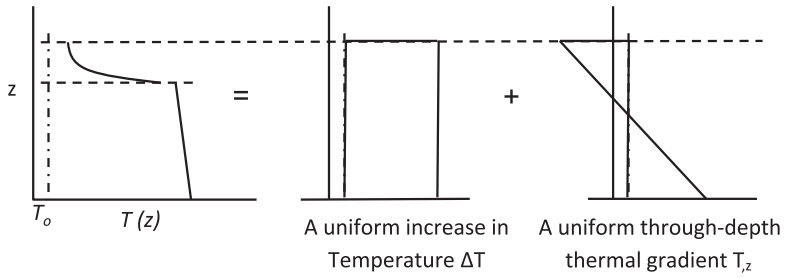

Fig. 7. Temperature distribution idealised as a uniform temperature increase and a through-depth thermal gradient.

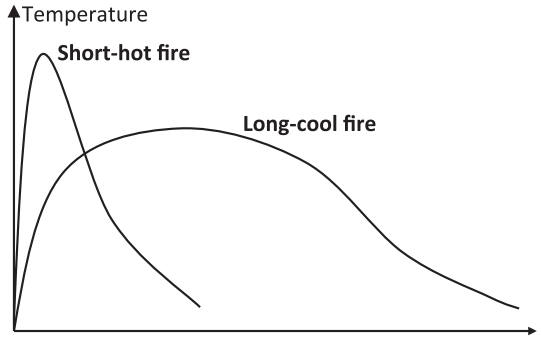

Fig. 8. Short-hot and long-cool fire.

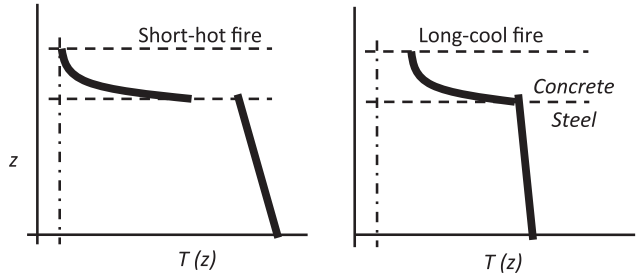

Fig. 9. Thermal response of sections to a short-hot and a long-cool fire.

The derivation of this is outlined in more detail in other articles [35,36] however for this instance a 2-dimensional variant is used as briefly discussed in [31]. In summary, the method is based on the steel within the floor system providing a catenary support to the applied loading, assuming that the ends are fully restrained against translation but not rotation and ignoring any capability of the concrete within the floor to provide any load resistance. This methodology has three stages:

1. Calculation of the temperature distribution through the depth of the member
2. Calculation of the deflected shape of the member, based upon the gross cross-sectional area, and the stresses and strains in the reinforcing bars associated with this deflected shape and steel temperature
3. Calculation of the load carrying deflection and the internal and external work done to move from the thermal deflection to the required deflection, the internal work done is based on the steel reinforcement only and ignores any contribution from the concrete.

Applying the thermal loading to the section results in a thermal deflection, w_T. For a 1-way spanning slab of length L, this deflection can be calculated by solving the following cubic equation, Eq. (12), for w_T:

$$w_T^3 + \left(\frac{4I_{comp}}{A_{comp}} - \frac{4N^T L^2}{\pi^2 E_{ref} A_{comp}}\right) w_T + \frac{16M^T L^2}{\pi^3 E_{ref} A_{comp}} \tag{12}$$

where I_{comp} is the second moment of area and A_{comp} is the area of the composite section, E_{ref} is a reference modulus used to determine the section properties of the section, N^T is the thermal force and M^T is the thermal moment – all calculated per unit width of the section.

The strains in the bars at the thermal deflection consist of two components, the thermal strain as a result of the increase in temperature of the steel and the strain induced in the steel as a result of the deflected shape of the concrete in which it is embedded. The total strain is the sum of the thermal strain and the mechanical strain, Eq. (13):

$$\varepsilon_{tot} = \varepsilon_{mech} + \varepsilon_T \tag{13}$$

The total strain in the steel at the deflection w_T is the strain in the steel required to follow the deflected shape of the floor system and is given by:

$$\varepsilon_{tot} = \frac{w_T^2 \pi^2}{4L^2} \tag{14}$$

The mechanical strains are therefore obtained by substituting Eq. (14) into Eq. (13) and subtracting the thermal strain in the steel, αT_s, from the total strain:

$$\varepsilon_{mech} = \frac{w_T^2 \pi^2}{4L^2} - \alpha T_s \tag{15}$$

where L is the length of the floor system, α is the coefficient of thermal expansion of the steel and T_s is the temperature of the steel (assuming lumped capacitance for the steel in this analysis). The membrane stress in the steel is based upon the mechanical strain, and is given by:

$$\sigma = \frac{w_T^2 \pi^2 E_s}{4L^2} - E_s \alpha T_s \tag{16}$$

where E_s is the modulus of elasticity, which is temperature dependant, and T_s the temperature of the steel.

These equations describe the mechanical state of the steel while under thermal loading only. To determine the state of the steel under the mechanical loading, a virtual work equation is applied and the internal and external work are compared while the total deflection is increased stepwise.

Based on the deflected shape, the external work done by a one way spanning slab moving a load p through a deflection is given by:

$$\Pi_{ext} = p \int_0^L \Delta w \frac{4LB}{\pi^2} \tag{17}$$

The internal work done at each step in the calculation is determined by evaluating the integral of the stress–strain diagram of the steel for the volume of steel in the floor system:

$$\Pi_{\text{int}} = \sum_{\forall st} \int^{V} \Delta\sigma_{st}\Delta\varepsilon_{st} dV \tag{18}$$

In order to calculate the deflection required to carry the load, w_p, the deflection should be increased incrementally and the total deflection should be substituted for w_T in Eqs. (17) and (18). The internal and the external work should then be compared to determine p, the load carried at the current deflection. If the calculated p is less than the applied load then the deflection should be increased.

3.2.3. Engineering demand parameter example

Using the methodology described above for the structural analysis it is proposed to declare the total deflection required to carry the load as the engineering demand parameter. This is analogous to an engineering demand parameter commonly used for PEER PBEE, which is inter-storey drift.

Details of the structure are as follows: the sub-assembly is a composite steel concrete section comprising a primary beam, section 305 × 165 × UB40, underneath a ribbed concrete deck with minimum thickness 70 mm at the troughs and maximum thickness at the ribs of 130 mm; reinforcing steel in the analysis is assumed to comprise of only the A193 anti-cracking mesh within the floor.

The floor assembly is located in the corner compartment of the building and is restrained at one end by the floor plate and structure in the adjacent bays and at the other end by a perimeter beam and column assembly. The location of the assembly in the floor plate of the building is shown in Fig. 10.

The general arrangement of the structural model, including the boundary conditions is shown in Fig. 11. The anti-cracking mesh is assumed to be located at mid – height of the floor and, for the purposes of the 1-dimensional analysis, the width of the concrete portion of the section is assumed to be given by ¼ of the effective length, in accordance with Eurocode 4 [37].

In order to evaluate the engineering demand parameter and to derive the corresponding hazard curve, the cumulative distributions of the engineering demand parameter need to be integrated with respect to the probability of exceedance of the intensity measure, as defined earlier in Eq. (3).

Fig. 12 shows the individual records of the Engineering Demand Parameters for the sample of fires. In this instance, the sample is the same set of fires which were used to derive the intensity measure curve in the previous section. The left hand plot is the intensity measure plotted against the annual probabilities of exceedance, and the right hand plot is the intensity measure plotted against the engineering demand parameter – the right hand plot shows all of the records of the engineering demand parameter. Fig. 12 also shows schematically an example of a discrete distribution of $P(EDP|IM)$.

In order to determine the hazard curve for the engineering demand parameter, the integral in Eq. (3) is evaluated numerically. For the range of intensity measures, the density function $p(EDP)$ is estimated assuming that it is an extreme value distribution and the $P(EDP|IM)$ is determined. This is then integrated with respect to $g(IM)$. Fig. 13 shows the resulting hazard curve of the total deflection.

3.3. Loss domain

Although the damage measures (DMs) provide a means to quantify the damage done to the structure they may also be used to quantify the damage to services, internal finishes and contents of the compartment. These aspects are not included in the analysis as it is anticipated that the smoke/heat damage to these from any fully developed fire would be complete requiring replacement regardless of the repairability of the structure.

A fragility function was assumed based on the EDP to categorise the level of damage done to the composite beam caused by a given value of an EDP. In each case there are three levels of damage, DM0, DM1 and DM2. The element is in DM0 when the level of the EDP is insufficient to cause any damage to the structure. The element enters DM1 when the EDP rises to a level where damage is caused to the element, but it is not beyond repair. DM2 applies when the EDP is such that the element is subject to damage which may require its replacement or there is local collapse. In the future, when more information becomes available regarding potential losses resulting from structural damage and the damage states are more rigorously defined, additional damage states and real (as opposed to assumed) fragility functions may be included to give a more realistic and complete estimate of the losses.

For the definition of the damage states associated with thermal deflection of the floor, the residual deflection of the floor following fires is considered. It is observable in the reports of the Cardington tests [38] as well as other reported tests on pre-stressed and composite floor slabs in fire [39] that following heating up to ¼ of the total deflection observed at the end of heating was recovered. Since cooling is not explicitly included within the analysis, the final thermal deflection at the end of the heating phase of the fire is taken as being the final deformation for determination of the damage measure later.

Since the recovery of the deflection during cooling would intuitively lead to a relaxation of the tensile forces observed in the steel reinforcement and in any steel beams present this is therefore seen as a conservative assumption at this stage.

The deflection limit for DM1 is assumed to be 30 mm, and the deflection limit for DM2 is assumed to be 130 mm. These are assumed values and are arbitrarily chosen. It is assumed that a deflection of up to 30 mm may be addressed without the requirement for considerable structural repair work since it is less than 1/3 of the total depth of the concrete section including the ribs and is given as the recommended deflection limit in Eurocode 2. Anything over 130 mm, which is equal to the total thickness of the concrete floor plate, is assumed to be irreparable and will require replacement. Standard deviations of both of these damage states are assumed to be 0.0001 mm.

Fig. 14 illustrates the conditional probabilities of the DM exceeding the damage state given a state of EDP, i.e. $P(DM|EDP)$.

The initial build cost for this part of the structure was calculated from the SCI document [28] and was then used to normalise the repair costs. The repair times have been estimated based on the repair work which is required. The repair times are normalised against the initial build time of the member, which is given as 5 days. Both the repair costs and the repair times have been assigned a lognormal distribution, the distributions of costs, repair times and damage states for reinforcement strain are summarised in Table 1 (for the lognormal distributions the mean values are given as a function of μ and σ, $mean = \exp(\mu + \sigma^2/2)$).

Fig. 15 below shows the cost consequence functions and repair time consequence functions associated with damage states of the reinforcement strain.

To illustrate the consequence functions a vector of EDP values may be taken and a random sample of costs may be taken for each of the EDPs to show the variation of the associated costs or downtimes. One such illustration of the consequence as a result of total deflection is shown in Fig. 16. The transition from one damage state to another, from DM0 to DM1 and subsequently from DM1 to DM2 is clearly visible in the figure for both downtime and con-

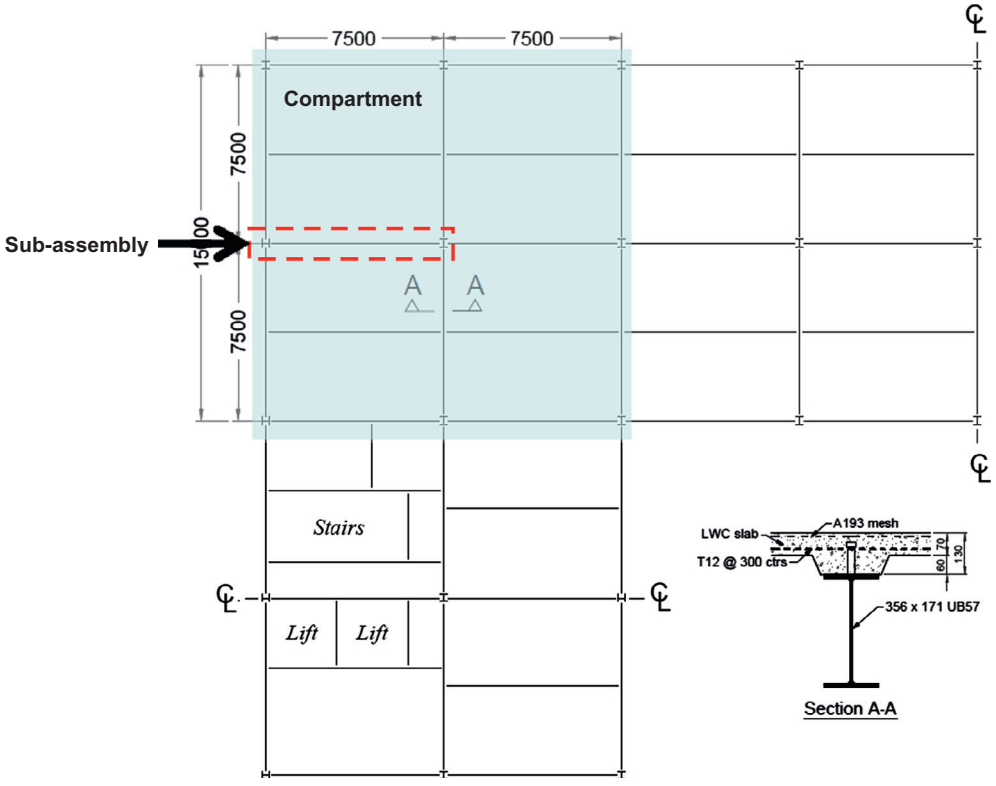

Fig. 10. Floor plate showing the location of the assembly.

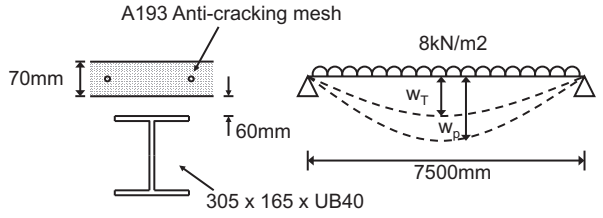

Fig. 11. General layout of the structural model showing the thermal and total deflections.

sequential cost as a result of the EDP. The variation in the consequence is also clearly visible as the scatter of the costs and downtimes.

The mean loss curves which reflect the damage measures are the mean values of the scatter illustrated in Fig. 16. The stepwise function which provides the curves may be obtained from the values provided in Table 1. This is possible due to the low level of variance assigned to the limits between the damage states.

The decision variables (DVs) are the final outputs from the PEER framework. They are a quantification of the likely mean annual losses incurred as a result of an event, in this case fire, leading to an unknown level of structural damage. Each DV is probabilistically related to a DM and each DM may have multiple DVs associated with it. The types of losses which may be measured as DVs are repair costs, repair times or casualties/injuries. The preceding analysis examined the effects of the fire on the structure only and be-

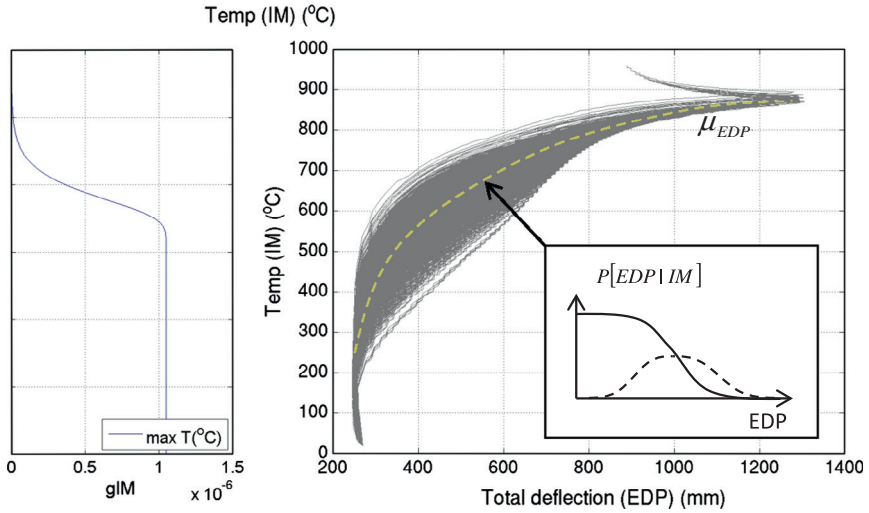

Fig. 12. Individual records of thermal deflection against compartment temperature (right hand graph) plotted alongside intensity measure hazard curves (left hand curve).

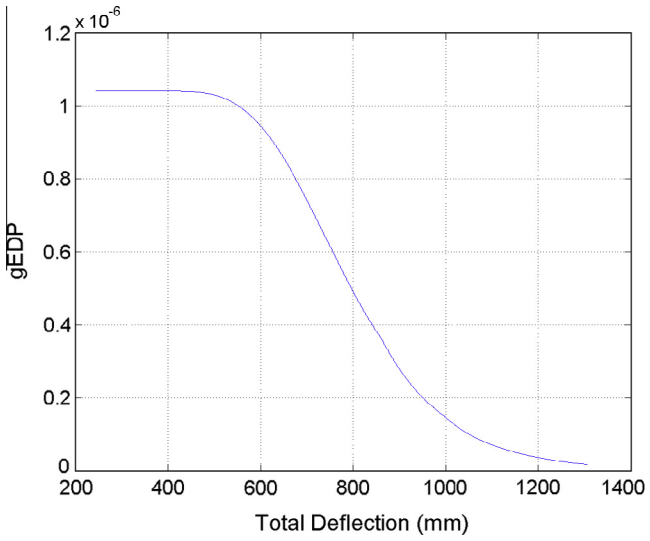

Fig. 13. Total deflection hazard curve.

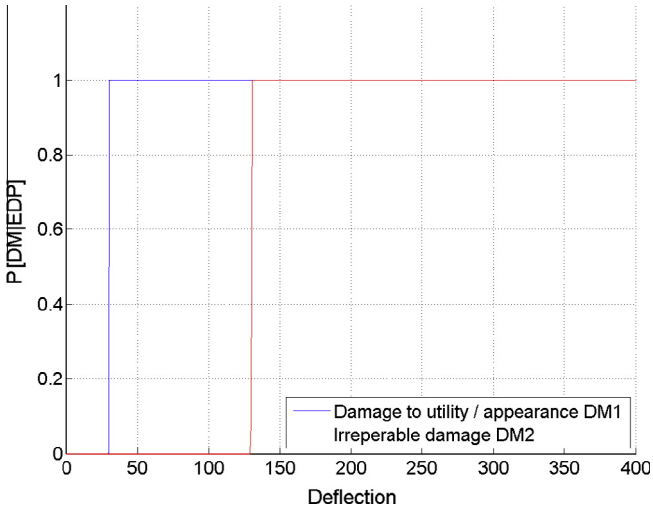

Fig. 14. Fragility function of the deflection of the composite assembly.

Table 1
Summary of assumed damage states, assumed repair times and assumed repair costs. 4 Decision variables (DVs) are given, 2 each describing the repair time and repair cost associated with the two damage measures.

	μ	σ	Distribution type
DM1	30	0.0001	Normal
DM2	130	0.0001	Normal
Repair time (DM1)	1.120	0.3	Lognormal
Repair time (DM2)	2.403	0.3	Lognormal
Repair cost (DM1)	−1.311	0.3	Lognormal
Repair cost (DM2)	0.519	0.3	Lognormal

cause of this the repair costs and repair times have been calculated solely for the structure of the building.

By integrating the Decision Variable and the Damage Measure resulting from an EDP with respect to the probability of the EDP occurring, as shown in Section 3.2, the frequency of exceeding a value of loss, or a period of downtime per year can be estimated. The integral to be evaluated is:

$$gDV = \int P(DV|EDP)dgEDP \tag{19}$$

Eq. (19) defines the annual occurrence of a decision variable measure, *gDV* as the conditional probability of exceeding a decision variable given that a damage measure has occurred, which is in turn given the occurrence of an engineering demand parameter. This is integrated over the annual occurrence of the demand parameter, *gEDP*. In order to evaluate Eq. (19) numerically, the probability of exceeding a given decision variable, *P*(*DV*|*EDP*) must be determined. Recognising that *DM1* is exclusive of *DM2* but *DM2* is not exclusive of *DM1*, for the stepwise damage measure described above, this is given by:

$$P(DV|EDP) = P(DV|DM1)P(DM1|\overline{DM2}, EDP) + P(DV|DM2)P(DM2|EDP) \tag{20}$$

where $P(DM1|\overline{DM2})$ denotes the probability of damage measure 1 occurring given that damage measure 2 has not occurred. Eq. (19) may therefore be evaluated numerically to obtain the annual costs and downtimes associated with the engineering demand parameter discussed.

Fig. 17 shows the cost and downtime curves associated with the total deflection.

The annual frequency of incurring any loss is consistently set to around 1×10^{-6}. This is the annual frequency of any of the events shown throughout the analysis for each of the stages of the framework and is the result of the initial probabilistic calculation of the likelihood of a structurally significant fire starting.

3.4. Protected steel example

In order to better understand the implications of the framework, a similar example is carried out assuming the steel frame is to be protected. In this instance, the structural model is revised slightly to account for the increased rigidity of the floor assembly, i.e. the deflection is calculated assuming flexure is the dominant load transfer mechanism, as opposed to catenary action.

The method used for determining the structural response for the EDP based on the protected structure is as follows. Firstly, calculate the horizontal end reaction forces and then the associated displacements. The total displacement should be based on a combination of: the bending displacement taking account of thermo-mechanical loading as well as the mechanical loading; the P–δ deflection arising from the restraint forces and the bending displacement; and the post-buckling deflection where appropriate. The modulus of elasticity in this method is temperature dependent, consistent with Section 3.2.2. The floor system and boundary conditions are the same as shown in Fig. 11. The thermo-mechanical loading is based on the same sectional analysis as for Section 3.2.

The horizontal restraint force, at the ends of the floor should be based on the thermal expansion of the section, i.e.

$$P_h = EA(\varepsilon_T - \varepsilon_\phi) \tag{21}$$

where ε_ϕ is a notional contraction strain [40] given by:

$$\varepsilon_\phi = 1 - \frac{\sin L\phi/2}{L\phi/2}, \text{where } \phi = \alpha T_{,z} \tag{22}$$

The total vertical deflections from the thermo-mechanical loads and the mechanical loads may then be determined by:

$$w_{mech} = \frac{L}{2}\sqrt{\frac{1}{6\varepsilon_\phi}} - \sqrt{\frac{1}{6\varepsilon_\phi - 1}} + \frac{5qL^4}{384EI} \tag{23}$$

The combination of the deflection as a result of thermo-mechanical loads and the mechanical loads as well as the horizontal restraint reactions induces additional P–δ moments and deflections at the mid-span of the floor system. Based on the combined

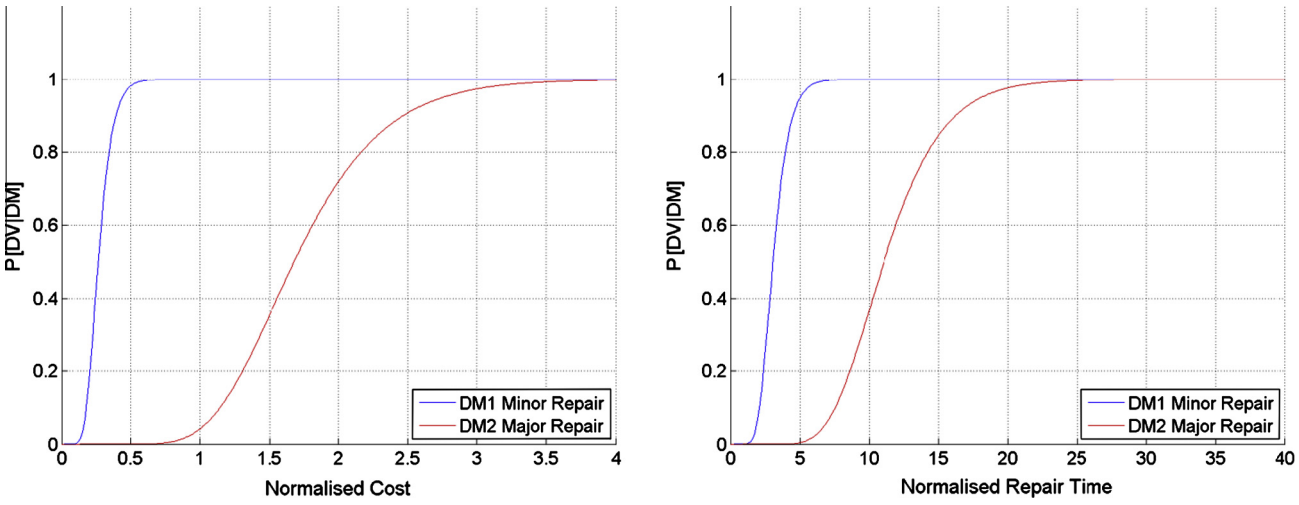

Fig. 15. Cost consequence functions and downtime consequence functions associated with damage states of total deflection.

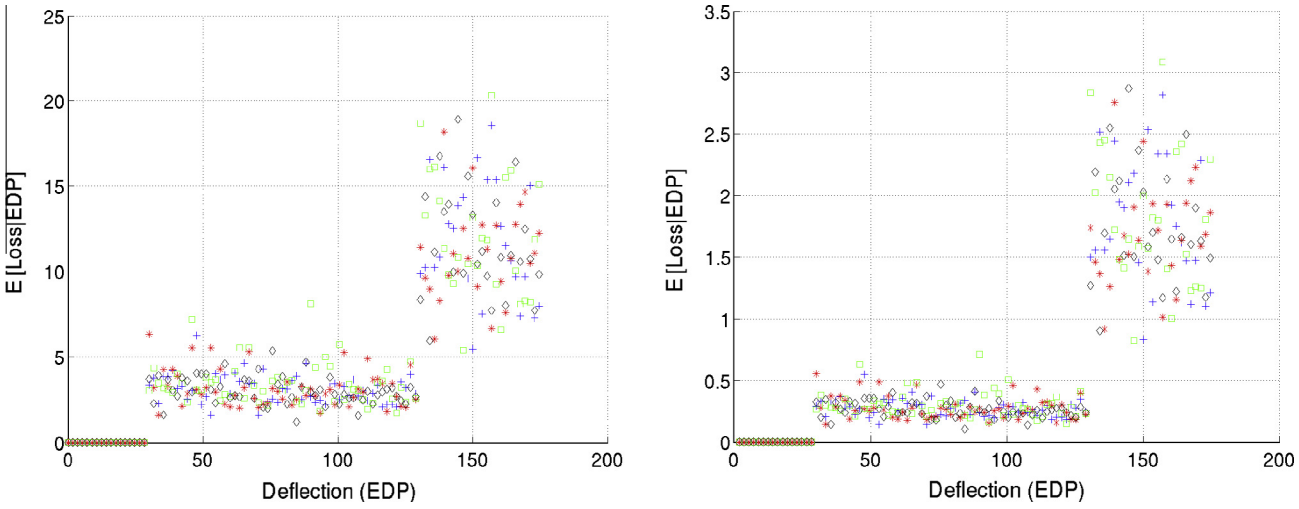

Fig. 16. Loss consequence and downtime consequence samples for total deflection as EDP.

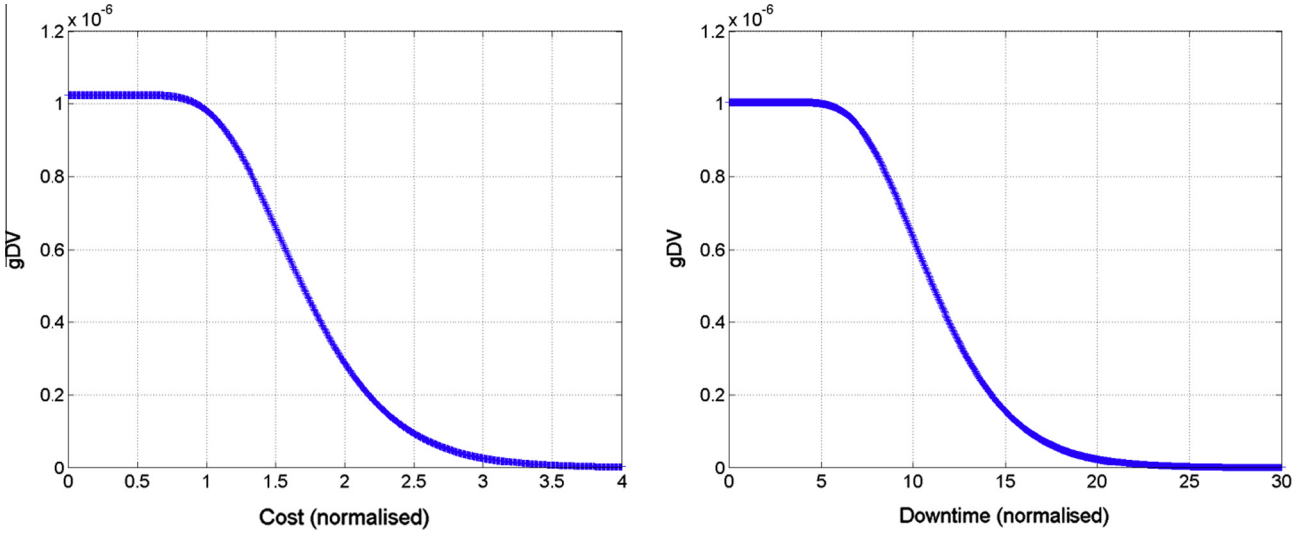

Fig. 17. Probabilistic annual repair cost and downtime associated with total deflection.

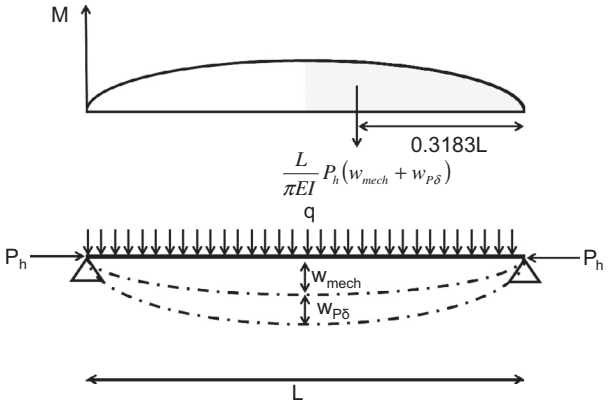

Fig. 18. Calculation of P–δ deflection.

deflections and the bending moment and the assumption that the deflected shape may be approximated as a sine curve, Fig. 18, the P–δ deflection may be derived as follows:

$$\frac{M}{EI}(x)=\frac{1}{EI}P_h(w_{mech}+w_{P\delta})\sin\frac{\pi x}{L} \tag{24}$$

Integrating this between $L/2$ and L gives the area of the M/EI diagram:

$$\int_{L/2}^{L}\frac{M}{EI}dx=\frac{L}{\pi EI}P_h(w_{mech}+w_{P\delta}) \tag{25}$$

By the moment area method, the moment of the M/EI diagram about the right hand end produces the deviation from the elastic curve. The centroid of the right half of the deflected shape is determined to be $0.3183L$, and therefore:

$$w_{P\delta}=\frac{L}{\pi EI}P_h(w_{mech}+w_{P\delta})0.3183L \tag{26}$$

Eq. (26) can be simplified to:

$$w_{P\delta}=\frac{Cw_{mech}}{1-C} \tag{27}$$

where $C=0.3183\dfrac{L^2P_h}{\pi EI}$

It should be noted that this is based on small deflection theory, and that the expression becomes invalid as P_h approaches an empirical limit of 10 times the Euler buckling load for a pin-ended member.

Finally, if appropriate the post-buckling deflection should be taken into account. The critical horizontal reaction may be calculated from:

$$P_{hcrit}=EA\alpha^{\pi 2}\Big/\alpha\lambda^2 \tag{28}$$

Here λ is the slenderness ratio of the composite section. If $P_h > P_{hcrit}$, then the post-buckling deflection must be taken into account.

The post-buckling deflection is given by:

$$w_{\sin\varepsilon_p}=\frac{2L}{\pi}\sqrt{\varepsilon_T-\varepsilon_\phi-\frac{\pi^2}{\lambda^2}} \tag{29}$$

From which the total deflection may be calculated:

$$w_{Total}=w_{mech}+w_{P\delta}+w_{\sin\varepsilon_p} \tag{30}$$

For comparison with the previous analysis, the intensity measure is as described above. The resulting records of total deflection, as well as the corresponding EDP hazard curve are shown in Fig. 19. The variance in the total deflection is considerably larger with the protected beam than with the unprotected beam. However the overall values of deflection are typically lower than with the unprotected beam, as would be expected. The derivation of the hazard curve is exactly the same as in the previous example. The only difference is in the means of calculating the engineering demand parameter.

Fig. 20 shows the resulting normalised cost and downtime curves for this example. Also plotted on Fig. 20 are the costs and downtimes for the unprotected beam examples for comparison.

3.5. Comparison

It is clear that the likely losses as a result of a fire with a protected structural assembly are considerably lower than if the structural assembly was unprotected. The likelihood of a loss greater than the initial build of the assembly is, for example around 0.9×10^{-6} for the unprotected assembly and 0.01×10^{-6} for the protected assembly. This is a considerably less likely event, as is the event of significant downtime for the adjacent structure. Leav-

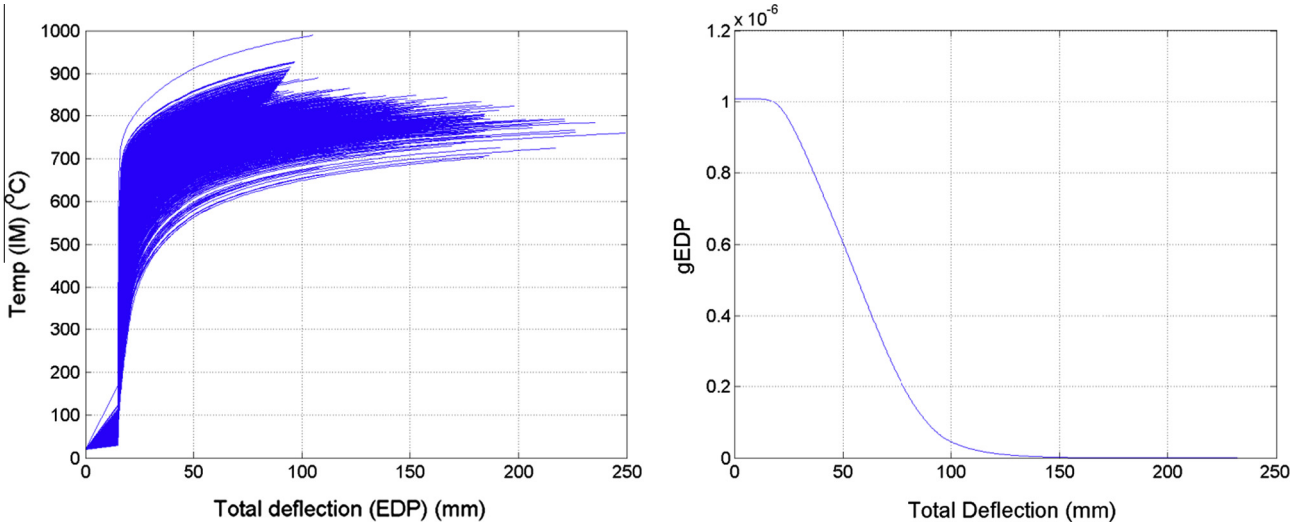

Fig. 19. Total deflection records and corresponding hazard curve for the example with steel protected.

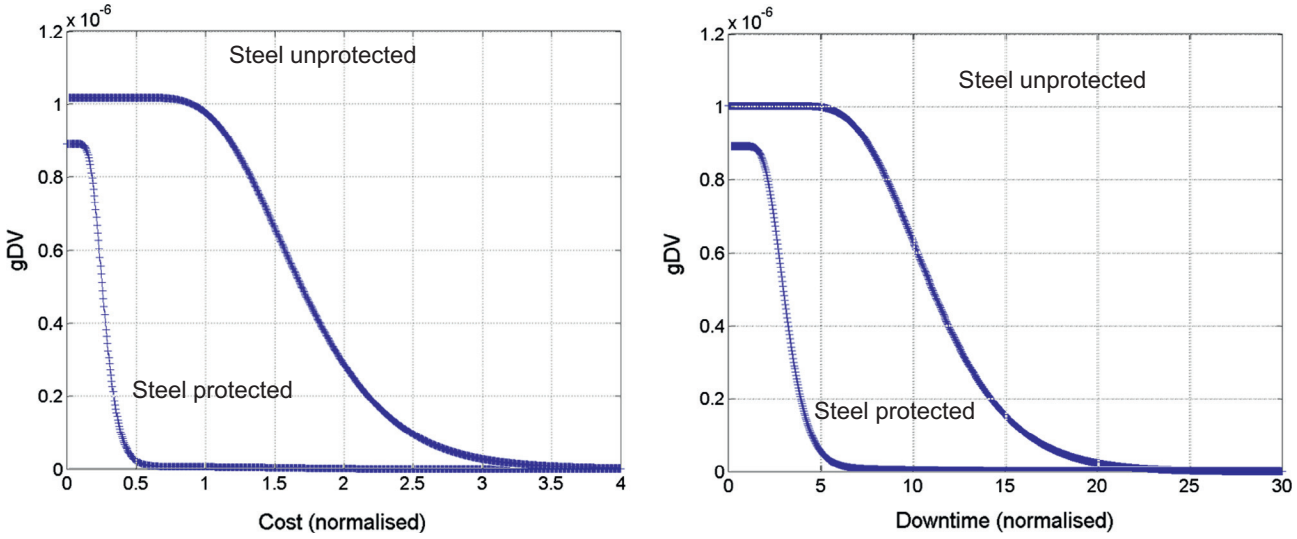

Fig. 20. Probabilistic annual repair cost and downtime associated with total deflection (protected beam example including unprotected beam).

ing structural steel unprotected in this instance therefore, as would intuitively be expected, increases the risk to the structure.

However, when the overall cost of the element of structure is considered then the economic benefits of protection become questionable. In the SCI publication, the cost for the structure is quoted as between £83 and £108/m^2 and the cost for protection between £12.70 and £32/m^2. Based on the frequency of costs to repair exceeding the initial build costs, the owner may budget a tiny per cent per annum of the build costs to repair the structure whereas protection could add as much as 38% to the cost of the structure. This obviously ignores the cost of room fittings, services and furnishings – however in the event of a structurally significant fire these are very likely to require repair or replacement regardless of the provision of structural protection.

This type of information may be used to influence decisions as to whether or not the structure should be protected, under the condition that it may be shown to sustain the applied load in fire for the duration of an analysis.

4. Discussion and conclusions

This paper has demonstrated an application of the PEER framework to structures in fire. The output of the analysis is a set of annual cost and downtime curves associated with one possible engineering demand parameter.

In keeping with the PEER framework, the triple integral of the PEER framework expression has been used in an unmodified state and therefore independence of the pinch variables has been assumed in the probabilistic calculations. However, the structural response is not independent from the fire model used and the potential fires which may occur and, the entire family of fire records which was developed for the IM calculation has been used to again determine the EDP distribution. This has led, in this example, to the requirement to employ simple hand calculation methods to obtain the 3000 large set of results which was deemed to provide a repeatable basis for the analysis.

A number of assumptions have been made in the paper, and the support for these will require considerable future research, in particular with reference to the repairability of fire damaged composite structures and the costs associated with this. There is little information in the literature and the majority of this is focussed on steel or concrete structures rather than composite construction. The material is also several years old and does not give any indication of the costs of repair. These are based in this paper upon the initial construction costs. Further information on damage states, the costs associated with the repair of fire damaged structures, as well as downtime associated with repair and the identification of alternative damage measures will most likely require a dialogue on this subject with industry.

An apparent disconnect between fire engineering and structural fire engineering provides reasonable justification at this time for the use of the parametric fire, however the impact of different fire models on the results of the framework should be considered in future research. The computational resources required to run numerous FE analyses to illustrate the application of the framework to Structural Fire Engineering have driven the authors to employ simpler analytical models in this paper although future iterations will consider different structural models which will allow the exploration of alternative EDPs and DMs.

The example presented has demonstrated the application of the PEER framework to structures in fire and the annual costs resulting from it may be used to better inform decisions on performance based structural fire engineering of buildings in the future as confidence in the framework increases.

References

[1] Tubbs B. ICC performance code for buildings and facilities – structural fire protection provisions. Structures 2001:1–9. http://dx.doi.org/10.1061/40558(2001)80.
[2] Anon. In: Proceedings of the Tianjin workshop on structural engineering for fire resistance, Part 2 performance based design. In: Tianjin workshop on structural engineering for fire resistance; 2002.
[3] Rini D, Lamont S. Performance based structural fire engineering for modern building design. Structures Congress, San Francisco; 2008. p. 1–12.
[4] Usmani A, Lange D, Webb A, Manohar CS, Sundar VS. Reliability of structural members subjected to fire. In: Fifth international ASRANet conference (ASRANet 2010), Edinburgh; 2010.
[5] Albrecht C, Hosser D. A risk informed framework for performance based structural fire protection according to the eurocode fire parts. In: 12th International fire science and engineering conference (Interflam 2010), Nottingham; 2010.
[6] EN 1990:2002 Eurocode – basis of structural design; 2002.
[7] Lange D, Usmani A, Torero J. A risk based framework for performance based fire safety design of steel and composite structures. In: Fifth international conference on advances in steel structures (Icass '07), Singapore; 2007.
[8] Frantzich H. Risk analysis and fire safety engineering. Fire Saf J 1998;31:313–29.
[9] Nilsson M, Ödén M. Metod för dimensionering av bärförmåga vid brand med riskanalys. Masters thesis, Lund University of Technology; 2007.
[10] Fahleson C, Johansson B, Lagerqvist O. Probabilistic design of steel structures in fire. Pro Development Sverige AB; 2009.

[11] Albrecht C, Hosser D. A response surface methodology for probabilistic life safety analysis using advanced fire engineering tools. In: 10th International symposium on fire safety science (IAFSS10), Karlsruhe; 2011.
[12] Hasofer A, Qu J. Response surface modelling of monte carlo fire data. Fire Saf J 2002;37:772–84.
[13] Stern-Gottfried J, Rein G. Travelling fires for structural design – Part I: literature review. Fire Saf J 2012;54:74–85.
[14] Stern-Gottfried J, Rein G. Travelling fires for structural design – Part II: design methodology. Fire Saf J 2012;54:96–112.
[15] PEER: Pacific Earthquake Engineering Research Center. <http://peer.berkeley.edu/>; 2011 [accessed 03.10.11].
[16] Porter KA. An overview of PEER's performance-based earthquake engineering methodology Keith A. Porter. In: Ninth international conference on applications of statistics and probability in civil engineering (ICASP9), San Francisco; 2003.
[17] Petrini F, Ciampoli M, Augusti G, Università S. A probabilistic framework for performance-based wind engineering. In: 5th European & African conference on wind engineering (EACWE 5), Florence; 2009.
[18] Hamburger RO, Whittaker AS. Considerations in performance-based blast resistant design of steel structures. In: Proceedings of AISC-SINY symposium on resisting blast and progressive collapse, New York, USA, December 4–5; 2003.
[19] Barbato M, Petrini F, Unnikrishnan VU, Ciampoli M. Performance-based hurricane engineering (PBHE) framework. Struct Saf 2013;45:24–35.
[20] Deierlein GG, Hamilton S. Framework for structural fire engineering and design methods; 2003.
[21] Baker JW, Cornell CA. PACIFIC EARTHQUAKE ENGINEERING vector-valued ground motion intensity measures for probabilistic seismic demand analysis vector-valued ground motion intensity measures for probabilistic seismic demand, analysis; 2006.
[22] Deierlein GG, Krawinkler H, Cornell CA. A framework for performance-based earthquake engineering. In: 2003 Pacific conference on earthquake engineering, New Zealand Society for Earthquake Engineering; 2003. p. 1–8.
[23] Koo SH. Forecasting fire development with sensor-linked simulation. PhD thesis, The University of Edinburgh; 2010.
[24] BS EN 1991-1-2:2002. Eurocode 1: Actions on structures - Part 1–2: General actions-actions on structures exposed to fire, (2002).
[25] IMPLEMENTATION OF EUROCODES – Handbook 5 – design of buildings for the fire situation, Leonardo da Vinci Pilot Project CZ/02/B/F/PP-134007; 2005.
[26] Lungu D, Rackwitz R. Joint Committee on Structural Safety – Probabilistic model code, Part 2: load models; 2001. <http://www.jcss.byg.dtu.dk/Publications/Probabilistic_Model_Code.aspx>.
[27] Schleich JB. Valorisation project: natural fire safety concept; 2001.
[28] Hicks SJ, Lawson RM, Rackham JW, Fordham P. Comparative structure cost of modern commercial buildings. 2nd ed. Ascot, Berkshire: The Steel Construction Institute; 2004.
[29] Lamont S, Usmani AS, Gillie M. Behaviour of a small composite steel frame structure in a "long-cool" and a "short-hot" fire. Fire Saf J 2004;39:327–57.
[30] Usmani AS. Understanding the response of composite structures to fire. In: North American steel construction conference, Baltimore; 2003.
[31] Cameron NJK. The behaviour and design of composite floor systems in fire. The University of Edinburgh; 2003.
[32] EN 1993-1-2:2005 Eurocode 3: design of steel structures Part 1.2 General rules – structural fire design; 2005.
[33] EN 1992-1-2: 2004 Eurocode 2: design of concrete structures – Part 1–2: general rules – structural fire design, 3; 2004.
[34] Drysdale D. An introduction to fire dynamics. 2nd ed. John Wiley & Sons, Ltd.; 1998.
[35] Cameron NJK, Usmani AS. New design method to determine the membrane capacity of laterally restrained composite floor slabs in fire Part 1: theory and method. Struct Eng 2005:28–33.
[36] Cameron NJK, Usmani AS. A new design method to determine the membrane capacity of laterally restrained composite floor slabs in fire Part 2: validation. Struct Eng 2005:34–9.
[37] BS EN 1994-1-1:2004. Eurocode 4: design of composite steel and concrete structures – Part 1-1: general rules and rules for buildings, 122; 2004.
[38] Martin D, Moore D. The behaviour of multi-storey steel framed buildings in fire. British Steel plc.; 1999. ISBN 0 900206 50 0.
[39] Ashton L. Fire research note no. 54 – prestressed concrete during and after fires, comparative tests on concrete floors in prestressed and reinforced concrete; 1953.
[40] Usmani A, Rotter J, Lamont S, Sanad A, Gillie M. Fundamental principles of structural behaviour under thermal effects. Fire Saf J 2001;36:721–44.